


Dissipative phase transitions in optomechanical systems

Fatemeh Bibak ^{1,2} Uroš Delić,¹ Markus Aspelmeyer,^{1,2} and Borivoje Dakić^{1,2}

¹Vienna Center for Quantum Science and Technology, Faculty of Physics, University of Vienna, Boltzmannngasse 5, 1090 Vienna, Austria

²Institute for Quantum Optics and Quantum Information Vienna, Austrian Academy of Sciences, Boltzmannngasse 3, 1090 Vienna, Austria



(Received 22 August 2022; revised 11 April 2023; accepted 12 April 2023; published 8 May 2023)

We show that optomechanical quantum systems can undergo dissipative phase transitions within the limit of a small nonlinear interaction and strong external drive. In such a defined thermodynamical limit, the nonlinear interaction stabilizes optomechanical dynamics in strong- and ultrastrong-coupling regimes. As a consequence, optomechanical systems possess a rich phase diagram consisting of periodic orbits and discontinuous and continuous dissipative phase transitions with and without bifurcation. We also find a critical point where continuous and discontinuous dissipative phase transition lines meet. Our analysis demonstrates that optomechanical systems are valuable for understanding the rich physics of dissipative phase transitions and ultrastrong-coupling regimes.

DOI: [10.1103/PhysRevA.107.053505](https://doi.org/10.1103/PhysRevA.107.053505)

I. INTRODUCTION

One of the recent research foci in the field of open quantum systems is the so-called dissipative phase transition (DPT) [1]. It is defined as an effect of the abrupt change in the physical properties of the steady state caused by small variations of the system's external parameters in the appropriate thermodynamic limit. Unlike their equilibrium counterparts, which can be divided into two distinct categories based on the nature of the fluctuations (thermal and quantum phase transitions), DPTs generally support the coexistence of thermal and quantum fluctuations [2], which leads in general to richer phase diagrams. Dissipative phase transitions are typically accompanied by intriguing phenomena [3–14], such as critical slowing down [15], optical bistability [16], and breakdown of photon blockade [17]. Some of these effects have been experimentally studied in a variety of physical systems [18–23].

In the context of optical quantum systems, recent developments in control and manipulation, as well as their interaction with the environment, make them good candidates for simulating the physics of many-body systems and quantum phase transitions [24–31]. A fundamental distinction between phase transitions in quantum optical systems and conventional phase transitions arises from the notion of the thermodynamic limit. The latter is usually associated with the limit of a large number of particles: Only in this regime can one observe a phase transition. While phase transitions in quantum optical systems can fall into this category, e.g., the Dicke model [32,33], the observation of phase transitions is possible even with a finite number of components due to their infinite-dimensional Hilbert spaces [34,35]. In this paper we follow this line of research and show that two coupled quantum harmonic oscillators exhibit a very rich phase diagram encompassing all known types of DPTs. A physical system exemplified in detail is the dissipative optomechanical system driven by an external laser field [36]. The interplay between the weak nonlinear interaction and a strong external drive (in the exact thermodynamical limit) results in linear dynamics with various steady states associated with different phase-space regions. The stability diagram identifies these regions and their

separation is marked by transition lines at which dissipative phase transitions occur. This is in contrast to a simplified standard linearized optomechanical approach, where the system dynamics is considered to be unstable beyond the transition lines [37–39]. Here we demonstrate that stabilization of the system is possible through the dissipative phase transitions in the whole red-detuned regime and partially in the blue-detuned regime. Our analysis reveals a rich phase diagram composed of discontinuous DPTs, continuous DPTs, and periodic orbits. The continuous DPT appears in two distinct categories: with and without bifurcation. We find a single critical point where bifurcation occurs in complete analogy to the continuous phase transition with symmetry breaking. The continuous DPT without bifurcation (symmetry breaking) is a curious effect that has only very recently been studied theoretically in nonequilibrium quantum systems [40]. To confirm the quantum properties of DPTs, we provide a numerical study and show that quantum entanglement and squeezing are maximized along transition lines, thus correctly marking the phase transition. Finally, we specify the universality class of the optomechanical systems by studying finite-size scaling and critical exponents.

II. QUANTUM OPTOMECHANICS IN THE THERMODYNAMIC LIMIT

Thermodynamic limit. A generic quantum optomechanical system consists of a laser-driven optical cavity with a movable mirror. The Hamiltonian of the system is typically of the following form [41] (with $\hbar = 1$):

$$H = \omega_c a^\dagger a + \omega_m b^\dagger b + g_0 a^\dagger (a + b^\dagger) - i(E^* e^{i\omega_L t} a - E e^{-i\omega_L t} a^\dagger). \quad (1)$$

Here a is the annihilation operator of the cavity mode with frequency ω_c and b is the annihilation operator of the mechanical resonator mode with frequency ω_m . The coupling rate between the cavity field and the mechanical resonator is denoted by g_0 , and E is the amplitude of the laser drive. Without loss of generality, we assume E is a real number. In the frame rotating

with the laser frequency ω_L , the Hamiltonian becomes time independent,

$$H = -\Delta a^\dagger a + \omega_m b^\dagger b + g_0 a^\dagger a (b + b^\dagger) - iE(a - a^\dagger), \quad (2)$$

where $\Delta = \omega_L - \omega_c$ is the detuning. The Markovian open system¹ is described by a time-independent master equation

$$\dot{\rho} = \mathcal{L}[\rho] = -i[H, \rho] + \kappa \mathcal{D}[a]\rho + \gamma \mathcal{D}[b]\rho, \quad (3)$$

where κ and γ are the damping rates of the cavity and the mechanical resonator, respectively, and $\mathcal{D}[o]\rho = 2o\rho o^\dagger - \rho o^\dagger o - o^\dagger o \rho$ is the Lindblad operator.

We begin our analysis by changing the picture $\rho \mapsto U(t)\rho U^\dagger(t)$, with

$$U(t) = \exp[\alpha^*(t)a - \alpha(t)a^\dagger] \exp[\beta^*(t)b - \beta(t)b^\dagger] \quad (4)$$

the displacement operator and $\alpha(t)$ and $\beta(t)$ yet to be determined. The master equation (3) keeps the form in the new picture with the new Lindblad operator $\mathcal{L}'[\rho] = -i[H(t), \rho] + \kappa \mathcal{D}[a]\rho + \gamma \mathcal{D}[b]\rho$ and the new time-dependent Hamiltonian, which we split into three terms

$$H(t) = H^{(1)}(t) + H^{(2)}(t) + H_{\text{int}}. \quad (5)$$

These are

$$H^{(1)}(t) = i\{\dot{\alpha}^* + [i\Delta - ig_0(\beta + \beta^*) + \kappa]\alpha^* - E\}a + i\{\dot{\beta}^* - (i\omega_m - \gamma)\beta^* - ig_0|\alpha|^2\}b + \text{H.c.}, \quad (6)$$

$$H^{(2)}(t) = -(\Delta - g_0\beta - g_0\beta^*)a^\dagger a + \omega_m b^\dagger b + g_0(\alpha^* a + \alpha a^\dagger)(b + b^\dagger), \quad (7)$$

$$H_{\text{int}} = g_0 a^\dagger a (b + b^\dagger). \quad (8)$$

Here we omit the explicit time dependence $\alpha = \alpha(t)$ and $\beta = \beta(t)$ for simplicity. Operators a and b are small quantum fluctuations around $\alpha(t)$ and $\beta(t)$. Our goal is to show that only the quadratic term $H^{(2)}(t)$ survives in the thermodynamic limit, leading to an exact linear dynamics of the system. The necessary precondition is that the linear term vanishes, i.e., $H^{(1)}(t) = 0$, which gives the set of equations for $\alpha(t)$ and $\beta(t)$:

$$\dot{\alpha}(t) = \{i\Delta - ig_0[\beta(t) + \beta^*(t)] - \kappa\}\alpha(t) + E, \quad (9)$$

$$\dot{\beta}(t) = -(i\omega_m + \gamma)\beta(t) - ig_0|\alpha(t)|^2. \quad (10)$$

These are the semiclassical equations of motion. We define the thermodynamic limit (TDL) as

$$E \rightarrow \infty, \quad g_0 \rightarrow 0 \quad \text{s.t.} \quad \tilde{E} = g_0 E \rightarrow \text{const.} \quad (11)$$

Given the first condition $E \rightarrow \infty$, the solution to the semiclassical equations (9) are not well defined, since in this case we get $\alpha(t) \rightarrow \infty$ and $\beta(t) \rightarrow \infty$. However, multiplying (9) with the interaction constant g_0 from both sides, we obtain

$$\begin{aligned} \dot{\tilde{\alpha}}(t) &= \{i\Delta - i[\tilde{\beta}(t) + \tilde{\beta}^*(t)] - \kappa\}\tilde{\alpha}(t) + \tilde{E}, \\ \dot{\tilde{\beta}}(t) &= -(i\omega_m + \gamma)\tilde{\beta}(t) - i|\tilde{\alpha}(t)|^2, \end{aligned} \quad (12)$$

where $\tilde{\alpha}(t) = g_0 \alpha(t)$ and $\tilde{\beta}(t) = g_0 \beta(t)$ represent the rescaled mean amplitudes of the cavity field and the mechanical resonator of the steady state. This is directly measurable in the experiment [42] and used by default in theoretical analysis. These equations now have well-defined solutions in the limit $E \rightarrow +\infty$ for $\tilde{\alpha}(t)$ and $\tilde{\beta}(t)$ only if $g_0 \rightarrow 0$ and $\tilde{E} = g_0 E \rightarrow \text{const}$ (see I in [43]). This choice of (11) is also in analogy to statistical mechanics, e.g., the TDL for a gas with n particles confined in a volume V is reached as $n \rightarrow \infty$ and $V \rightarrow \infty$, keeping the density N/V constant. Following this analogy in optomechanical systems, we have the mean photon number in the cavity $n \propto E$ and the length of the cavity $L \propto 1/g_0$ [36], which is then consistent with the choice of the TDL (11).

Once we set the condition (11), the displaced nonlinear interaction term (8) $H_{\text{int}} = g_0 a^\dagger a (b + b^\dagger) \rightarrow 0$ vanishes as $g_0 \rightarrow 0$, while the only term that survives in the limit is the quadratic Hamiltonian (7) as a function of $\tilde{\alpha}(t)$ and $\tilde{\beta}(t)$. Thus, the dynamics becomes linear in the thermodynamical limit.

To study the steady-state properties, we take the limit $t \rightarrow +\infty$ for which Eqs. (12) can lead to stationary solutions $(\tilde{\alpha}_s, \tilde{\beta}_s)$ obtained by solving $\dot{\tilde{\alpha}}(t) = 0$ and $\dot{\tilde{\beta}}(t) = 0$, i.e.,

$$\begin{aligned} [i\Delta - i(\tilde{\beta}_s + \tilde{\beta}_s^*) - \kappa]\tilde{\alpha}_s + \tilde{E} &= 0, \\ -(i\omega_m + \gamma)\tilde{\beta}_s - i|\tilde{\alpha}_s|^2 &= 0. \end{aligned} \quad (13)$$

In this case, the Hamiltonian in (5) (and consequently the corresponding master equation) becomes time independent.

Semiclassical solutions. Before proceeding to the quantum regime, we will find the stationary solutions of the semiclassical equations (13). These are the set of coupled cubic equations which can be reduced to second order using the following ansatz. First, we define the rescaled mean photon number $\tilde{n} = |\tilde{\alpha}|^2$, which satisfies the equation

$$\left[\left(\Delta + \frac{2\tilde{n}\omega_m}{\omega_m^2 + \gamma^2} \right)^2 + \kappa^2 \right] \tilde{n} - \tilde{E}^2 = 0. \quad (14)$$

In general, there are three solutions to the cubic equation above; however, only those satisfying $\tilde{n} \geq 0$ are physical. It is well known that one solution, which we label \tilde{n}_1 , is always physical in the whole parameter space [36]. We set \tilde{n}_1 as the reference and the corresponding solutions of (13) we denote by $(\tilde{\alpha}_1, \tilde{\beta}_1)$, i.e., those satisfying $\tilde{n}_1 = |\tilde{\alpha}_1|^2$. On this basis, we define two key parameters, effective detuning and coupling strength:

$$\begin{aligned} \tilde{\Delta} &= \Delta - (\tilde{\beta}_1 + \tilde{\beta}_1^*), \\ G &= \sqrt{\tilde{n}_1} = |\tilde{\alpha}_1|. \end{aligned} \quad (15)$$

Having assumed that one solution of the cubic equation (14) is known (the parameter $\tilde{n}_1 = G^2$), we can find the analytical expression for the other two solutions

$$\begin{aligned} \tilde{n}_{2,3} &= \frac{1}{2}G^2 - \frac{\tilde{\Delta}}{2\omega_m}(\gamma^2 + \omega_m^2) \\ &\pm \frac{1}{2}\sqrt{G^4 - \frac{\kappa^2}{\omega_m^2}(\gamma^2 + \omega_m^2)^2 - 2G^2\frac{\tilde{\Delta}}{\omega_m}(\gamma^2 + \omega_m^2)}. \end{aligned} \quad (16)$$

¹The Markovian approximation can safely apply to optomechanical systems at room temperature.

Finally, the stationary solutions to the semiclassical equations (13) can be expressed solely in terms of the parameters $\tilde{\Delta}$ and G , i.e.,

$$\begin{aligned}\tilde{\alpha}_j &= \frac{iG\sqrt{\tilde{\Delta}^2 + \kappa^2}}{\tilde{\Delta} + \frac{2\omega_m(\tilde{n}_j - \tilde{n}_1)}{\omega_m^2 + \gamma^2} + i\kappa}, \\ \tilde{\beta}_j &= \frac{-|\tilde{\alpha}_j|^2}{\omega_m - i\gamma}, \quad j = 1, 2, 3.\end{aligned}\quad (17)$$

Each of these solutions, when substituted into (7), defines one Hamiltonian in the thermodynamical limit, i.e.,

$$H_j = -(\Delta - \tilde{\beta}_j - \tilde{\beta}_j^*)a^\dagger a + \omega_m b^\dagger b + (\tilde{\alpha}_j^* a + \tilde{\alpha}_j a^\dagger)(b + b^\dagger), \quad (18)$$

with $j = 1, 2, 3$. This is our working Hamiltonian in the thermodynamic limit, which has two new properties: (a) The detuning of the cavity mode is shifted to the value $\tilde{\beta}_j + \tilde{\beta}_j^*$ and (b) the interaction between the modes is linear and its strength is directly proportional to the amplitude $|\tilde{\alpha}_j|$. Moreover, these Hamiltonians depend only on the parameters $\tilde{\Delta}$ and G , which will serve to define our stability diagram. For example, the Hamiltonian for the reference solution

reads

$$H_1 = -\tilde{\Delta}a^\dagger a + \omega_m b^\dagger b + G(e^{i\theta(\tilde{\Delta})}a + e^{-i\theta(\tilde{\Delta})}a^\dagger)(b + b^\dagger), \quad (19)$$

with $\theta = \arg(\tilde{\alpha}_1) = \arg(\kappa + i\tilde{\Delta})$.

Stability analysis and the quantum steady state. In this section we examine the quantum-mechanical behavior of the system in the thermodynamic limit. To do this, we find the steady-state solution of the master equation

$$\dot{\rho} = \mathcal{L}[\rho] = -i[H_j, \rho] + \kappa\mathcal{D}[a]\rho + \gamma\mathcal{D}[b]\rho, \quad j = 1, 2, 3. \quad (20)$$

For simplicity, we use an equivalent formulation of the problem in terms of the Fokker-Planck equation for the Wigner quasiprobability distribution associated with the density operator ρ [44]. First, we introduce the cavity field quadratures $x_c \equiv (a + a^\dagger)/\sqrt{2}$ and $p_c \equiv (a - a^\dagger)/i\sqrt{2}$ and the mechanical resonator quadratures $x_m \equiv (b + b^\dagger)/\sqrt{2}$ and $p_m \equiv (b - b^\dagger)/i\sqrt{2}$. The Fokker-Planck equation in terms of quadrature vector in phase space $\vec{x} = (x_c, p_c, x_m, p_m)$ can be stated as

$$\partial_t W(\vec{x}, t) = (-\vec{\nabla}_A j \vec{x} + \frac{1}{2} \vec{\nabla}^T D \vec{\nabla}) W(\vec{x}, t), \quad (21)$$

with diffusion matrix $D = \text{diag}(\kappa, \kappa, \gamma, \gamma)$ and A_j the drift matrix which can be calculated directly from the Hamiltonian (18), i.e.,

$$A_j = \begin{pmatrix} -\kappa & -2\left[\frac{\omega G^2}{\omega^2 + \gamma^2} + \text{Re}(\tilde{\beta}_j)\right] + \tilde{\Delta} & 2\text{Im}(\tilde{\alpha}_j) & 0 \\ 2\left[\frac{\omega G^2}{\omega^2 + \gamma^2} + \text{Re}(\tilde{\beta}_j)\right] - \tilde{\Delta} & -\kappa & 2\text{Re}(\tilde{\alpha}_j) & 0 \\ 0 & 0 & -\gamma & -\omega_m \\ 2\text{Re}(\tilde{\alpha}_j) & -2\text{Im}(\tilde{\alpha}_j) & \omega_m & -\gamma \end{pmatrix}. \quad (22)$$

The drift matrix A_j controls the time evolution of the first moment $\langle x \rangle(t)$,

$$\frac{d\langle \vec{x} \rangle}{dt} = A_j \langle \vec{x} \rangle, \quad (23)$$

while the time evolution of the second moment, the correlation matrix V , is given by

$$\frac{dV}{dt} = A_j V + V A_j^T + D. \quad (24)$$

Since the dynamics is linear, the steady-state solution to Eq. (21) is a unique Gaussian state (provided the dynamics is stable):

$$W_s(\vec{x}) = \frac{1}{4\pi^2 \sqrt{\det V_s}} e^{(\vec{x} - \vec{x}_s)^T V_s^{-1} (\vec{x} - \vec{x}_s) / 2}. \quad (25)$$

Here x_s and V_s are stationary solution to Eqs. (23) and (24), respectively.

Each A_j (for $j = 1, 2, 3$) defines one steady-state solution, which we label with roman numerals I (reference), II, and III. We study their stability by considering the time evolution of a small deviation around the stationary solution

$$x = x_s + \delta x,$$

$$\frac{d\langle \delta x \rangle}{dt} = A_j \langle \delta x \rangle, \quad (26)$$

which has the time evolution $\langle \delta x \rangle(t) = e^{tA_j} \langle \delta x \rangle(0)$. The steady state is stable if all eigenvalues λ_i of A_j satisfy $\text{Re}(\lambda_i) < 0$ (more details about eigenvalues of the drift matrix can be found in II in [43]). Using this condition, we obtain the necessary and sufficient conditions for the stability of the solution, known as the Routh-Hurwitz criterion [45]:

$$\begin{aligned} & 4\gamma\kappa \left[(\gamma + \kappa)^2 + \left(2\frac{\omega_m G^2}{\omega_m^2 + \gamma^2} + \tilde{\beta}_i + \tilde{\beta}_i^* + \omega_m - \tilde{\Delta} \right)^2 \right] \\ & \times \left[(\gamma + \kappa)^2 + \left(-2\frac{\omega_m G^2}{\omega_m^2 + \gamma^2} - \tilde{\beta}_i - \tilde{\beta}_i^* + \omega_m + \tilde{\Delta} \right)^2 \right] \\ & + 16(\gamma + \kappa)^2 \omega_m |\tilde{\alpha}_i|^2 \left(2\frac{\omega_m G^2}{\omega_m^2 + \gamma^2} + \tilde{\beta}_i + \tilde{\beta}_i^* - \tilde{\Delta} \right) > 0, \end{aligned} \quad (27)$$

$$(\gamma^2 + \omega_m^2) \left[\kappa^2 + \left(2 \frac{\omega_m G^2}{\omega_m^2 + \gamma^2} + \tilde{\beta}_i + \tilde{\beta}_i^* - \tilde{\Delta} \right)^2 \right] - 4\omega_m |\tilde{\alpha}_i|^2 \left(2 \frac{\omega_m G^2}{\omega_m^2 + \gamma^2} + \tilde{\beta}_i + \tilde{\beta}_i^* - \tilde{\Delta} \right) > 0. \quad (28)$$

Instability occurs if at least one of the above inequalities is violated. This is closely related to the dissipative phase transition, which we will examine in the next section.

III. DISSIPATIVE PHASE TRANSITIONS

When an abrupt change in the physical properties of the steady state occurs (in the thermodynamic limit), we have a dissipative phase transition. Mathematically, this situation happens when the so-called Liouvillian gap closes [1]. More precisely, consider the solution of the eigenvalue problem of the operator in (20),

$$\mathcal{L}[e_k] = \mu_k e_k, \quad k = 1, 2, \dots \quad (29)$$

Given its specific form, one can show that all the eigenvalues satisfy $\text{Re}(\mu_k) \leq 0$, with $\mu_1 = 0$ the eigenvalue associated with the steady state [46,47]. For convenience, we sort the eigenvalues in such a way that $|\text{Re}(\mu_1)| < |\text{Re}(\mu_2)| < \dots$ and the relevant quantity is the Liouvillian gap $\mu = -\mu_2$. The DPT occurs when the real part of the gap vanishes, i.e., $\text{Re}(\mu) = 0$. For linear systems, this condition completely translates to a constraint on eigenvalues of the drift matrix [32,48], i.e., for eigenvalues of A_j sorted in order $|\text{Re}(\lambda_1)| < |\text{Re}(\lambda_2)| < |\text{Re}(\lambda_3)| < |\text{Re}(\lambda_4)|$, the DPT occurs for $\text{Re}(\lambda_1) = 0$. The last condition is precisely the Routh-Hurwitz criterion (27) and (28) defined in the preceding section. In this way, we establish a one-to-one correspondence between instability and dissipative phase transitions for our optomechanical system. The points for which the left-hand side of Eq. (27) vanishes are called hard-mode instabilities and correspond to the pure imaginary Lindblad gap $\text{Re}(\lambda_1) = 0$. In this regime the system exhibits periodic orbits [49]. On the other hand, the points for which the left-hand side of Eq. (28) vanishes are called soft-mode instabilities and correspond to the closure of the Lindblad gap, i.e., $\lambda_1 = 0$. In this regime the system undergoes first- and second-order dissipative phase transitions [1].

We investigate the stability of all three solutions and the results are shown in the phase (stability) diagram in Fig. 1. The diagram is composed of seven regions (described in detail in the caption of Fig. 1) separated by hard- (red lines) and soft-mode (blue and green lines) instability lines. Interestingly, we find stability in the ultrastrong-coupling regime (typically $G > 0.1\omega_m$), in the whole red-detuned regime and partially in the blue-detuned regime, where the stabilization is obtained via dissipative phase transition. This contrasts with the common belief that this regime has fundamental parametric instability (see II in [43]). Dissipative phase transitions occur at transition lines, and we divide them into several distinct categories:

First-order phase transition. First-order phase transitions or discontinuous phase transitions correspond to a discontinuous change in the behavior of an observable's mean

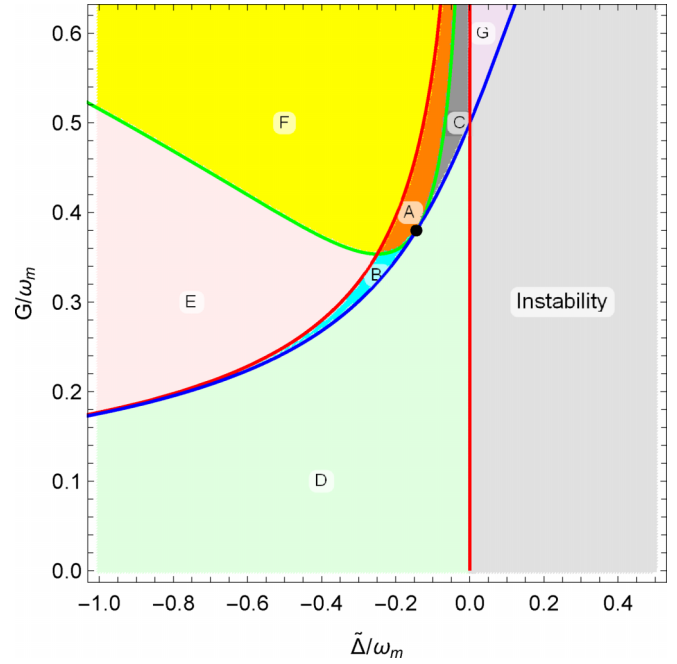


FIG. 1. Phase (stability) diagram. Optomechanical systems possess three distinct steady-state solutions which we label I (reference), II, and III. Based on the stability regions of these solutions, the stability diagram can be decomposed into seven regions (A–G). Two stable steady states coexist in regions A (II and III), B (I and III), and C (I and II). Only one stable steady-state exists in regions D (I), E (I), F (II), and G (II). The solutions are separated by instability lines: the hard mode (red) and the soft mode (blue and green) with one touching point (black dot, the critical point). For simplicity, the results are evaluated for $\kappa = \frac{1}{4}$ and $\gamma = 0$ in units $\omega_m = 1$. For other values the results do not change qualitatively.

values across the transition line. The typical behavior is shown in Fig. 2(a), where the rescaled mean photon number shows a discontinuous change. The optomechanical system exhibits a first-order phase transition along the blue soft-mode instability line (see Fig. 1). For $\tilde{\Delta}_c < \tilde{\Delta} < 0$ (with $\tilde{\Delta}_c/\omega_m = -1/4\sqrt{3}$) we have a first-order DPT between the steady states I and II, whereas for $\tilde{\Delta} < \tilde{\Delta}_c$ we have a first-order DPT between the steady states I and III. Notably, the latter occurs in the regime of parameters which is in the domain of experimental reach [38]. The first-order transition line separates bistable regions, i.e., B and C, from the monostable region D.

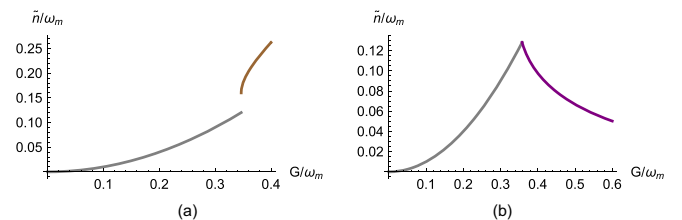


FIG. 2. Rescaled mean photon number \tilde{n} . (a) Discontinuous DPT between the I and the III steady state. (b) Continuous DPT between the I and the II steady state. The plots are evaluated for $\tilde{\Delta} = -0.2$, $\kappa = \frac{1}{4}$, and $\gamma = 0$ in units $\omega_m = 1$.

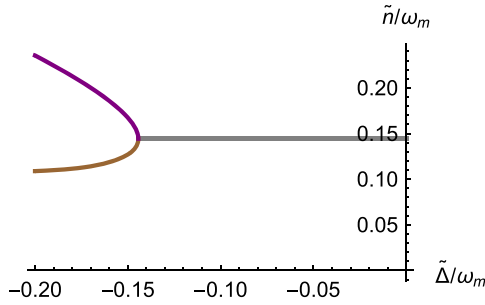


FIG. 3. Bifurcation diagram: the bifurcation in the rescaled mean photon number in the cavity at the critical point $(\tilde{\Delta}_c, G_c) = (-1/4\sqrt{3}, \sqrt{1/4\sqrt{3}})$, for $G = G_c$, $\kappa = 1/4$, and $\gamma = 0$ in units $\omega_m = 1$.

Typically, the system's state in these bistable regions depends on its history, which then gives rise to hysteretic behavior [36,50].

Second-order phase transition. Second-order or continuous phase transitions involve a continuous change in an observable's mean values across the transition line. The typical behavior is shown in Fig. 2(b), where the rescaled mean photon number displays a continuous change across the phase transition. In our system, the second-order DPT occurs along the soft-mode instability line where two different steady states in the thermodynamic limit are equal. We find two categories of continuous DPTs: with and without bifurcation. Dissipative phase transitions without bifurcation occur when the soft-mode instabilities of exactly two steady states are equal such that each of the solutions is stable on one side of the stability line. In our case, such a phase transition between the steady states I and III occurs along the green soft-mode instability line for $\tilde{\Delta} < \tilde{\Delta}_c < 0$ (see Fig. 1). Similarly, in the region defined by $\tilde{\Delta} < \tilde{\Delta}_c$ along the green instability line, we have another continuous DPT without bifurcation between the steady states I and II. The two soft-mode instability lines (blue and green) meet at the critical point $(\tilde{\Delta}_c, G_c)$, where

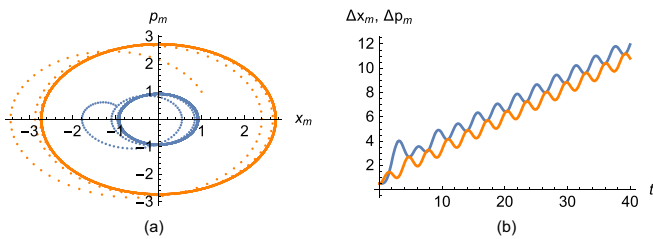


FIG. 4. Periodic orbits. The optomechanical systems exhibit periodic behavior along the hard-mode instability line (red lines in Fig. 1). (a) Mechanical phase space. The system dynamic is sensitive to the initial condition. Blue and orange orbits correspond to the initial conditions $(x_c, p_c, x_m, p_m) = (1, 1, -1, \frac{1}{2})$ and $(1, \frac{1}{2}, 1, 1)$, respectively. (b) Fluctuations in the mechanical resonator position (blue) and momentum (orange) growing linearly in time, indicating the instability of periodic orbits along the hard-mode instability line. The plots are calculated from the solutions of Eq. (24) for $V(0) = \mathbb{I}$, for $\kappa = \frac{1}{4}$, $\gamma = 0$, $\tilde{\Delta} = -1$, and $G = 1/4\sqrt{2}$ in units $\omega_m = 1$.

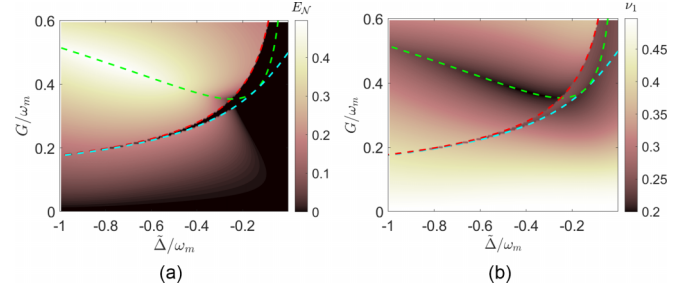


FIG. 5. Entanglement and squeezing. (a) Logarithmic negativity in the phase diagram. (b) Squeezing in the system as measured via the smallest eigenvalue of the correlation matrix in the phase diagram. The considered steady states in regions with more than one stable steady state are as follows (regions are defined in Fig. 1): A (III), B (III), and C (I). Here $\kappa = \frac{1}{4}$ and $\gamma = 0$ in units $\omega_m = 1$.

we have a continuous DPT with bifurcation. This behavior is depicted in Fig. 3.

Periodic orbits. The imaginary gap of the Liouvillian gives rise to the onset of oscillations, which do not have any counterpart in the closed system. These oscillations can be divided into limit cycles and periodic orbits [49]. Limit cycles are isolated trajectories, meaning all neighboring trajectories either converge to the limit cycle or diverge to another attractor. Stable limit cycles are accompanied by self-sustained oscillations and have been extensively studied in optomechanical systems [51–54]. In contrast, periodic orbits are surrounded by closed orbits and thus the amplitude of oscillations depends on the initial conditions. Optomechanical systems experience periodic orbits along the hard-mode instability lines. The typical behavior is shown in Fig. 4.

Quantum properties. An interesting question is the behavior of quantum properties such as entanglement and squeezing in different phases of the system. To answer this question, one must consider quantum fluctuations. In the thermodynamic limit, stable linear dynamics results in a Gaussian steady state, which is entirely characterized by its correlation matrix that is found as the stationary solution of Eq. (24).

To study entanglement between the mechanical and cavity modes we use Simon's criteria [55]. We employ logarithmic negativity as a measure of entanglement for continuous-variable systems, which is defined as $E_{\mathcal{N}} = \max[0, -\ln 2\eta^-]$ [56]. For a two-mode Gaussian state with a correlation matrix of the form

$$V = \begin{pmatrix} \alpha & \beta \\ \beta^T & \gamma \end{pmatrix}, \quad (30)$$

we have $\eta^- \equiv 2^{-1/2}[\Sigma(V) - \sqrt{\Sigma(V)^2 - 4 \det V}]^{1/2}$, where $\Sigma(V) \equiv \det \alpha + \det \gamma - 2 \det \beta$. A Gaussian state is entangled if and only if $\eta^- < \frac{1}{2}$. The typical behavior of the logarithmic negativity is shown in Fig. 5(a). Entanglement reaches a maximum value of $E_{\mathcal{N}} = \frac{1}{2}$ at the continuous DPT between steady states I and II, thus correctly marking the dissipative phase transition in the system.

Next we perform squeezing analysis in the phase diagram. A Gaussian state is called a squeezed state if there exists a basis in phase space in which at least one diagonal element of the

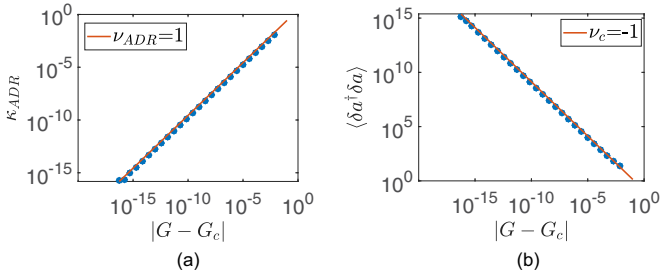


FIG. 6. Critical exponents. (a) Asymptotic decay rate κ_{ADR} in terms of $|G - G_c|$ in the log-log plot displaying power-law behavior near the continuous DPT point with exponent $\nu_{\text{ADR}} = 1$. (b) Mean fluctuations of photon number in the cavity $\langle \delta a^\dagger \delta a \rangle$ in terms of $|G - G_c|$ in the log-log plot exhibiting power-law behavior near the continuous DPT point with exponent $\nu_c = -1$. Both plots have been evaluated for $\kappa = \frac{1}{4}$, $\gamma = 0$, and $\tilde{\Delta} = \tilde{\Delta}_c$ in units $\omega_m = 1$.

correlation matrix is smaller than $\frac{1}{2}$ (shot-noise limit) [57]. We evaluate the diagonal elements of the correlation matrix in the (x_c, p_c, x_m, p_m) basis and we find all of them to be greater than $\frac{1}{2}$ in the whole phase space. This means that measurement of quadratures will not display squeezing effects at any point in the space of parameters. However, investigation of the lowest eigenvalue of the correlation matrix, presented in Fig. 5(b), reveals that there exist regions with eigenvalues less than $\frac{1}{2}$. This means that squeezing is present for a hybrid mode which involves combination of the cavity and mechanical mode.² As can be seen from the evaluated plot, the maximum squeezing also occurs at the continuous DPT line between steady states I and II. These calculations show that squeezing properly marks the phase transition. While squeezing changes continuously along continuous DPTs, it changes discontinuously along discontinuous DPTs. This observation shows that squeezing also reveals the nature of the DPTs.

Universality class. Universality is one of the remarkable properties of continuous equilibrium phase transitions [58] which originates from the long-range fluctuation close to the continuous phase transition point. In such cases, the correlation length becomes much larger than the typical range of the interactions, which results in the cooperative phenomena independent of the microscopic details of the considered system. Unlike for equilibrium phase transitions, little is known about nonequilibrium phase transitions due to the lack of a general framework for studying DPTs. Still, it is believed that nonequilibrium phenomena can be grouped into universality classes similar to equilibrium systems. As we have shown, the optomechanical system undergoes both continuous and discontinuous DPTs in the thermodynamic limit. To specify the universality class, we numerically compute the critical exponents of two quantities (see Fig. 6): photon-number fluctuations $\langle \delta a^\dagger \delta a \rangle \propto |G - G_c|^{\nu_c}$ and asymptotic decay rate (ADR) $\kappa_{\text{ADR}} \propto |G - G_c|^{\nu_{\text{ADR}}}$ (with $\nu_c = -1$ and $\nu_{\text{ADR}} = 1$), where the ADR determines the timescale at which the steady state is attained [59].

²The hybrid modes can be obtained by applying appropriate linear optical elements, e.g., beam splitters and phase shifters, to the cavity and mechanical modes.

Finally, we calculate the finite-size scaling of optomechanical systems with the Keldysh formalism [60,61] (see III in [43]), which gives rise to the following scaling relation for the photon number in the cavity:

$$\langle n_c \rangle \approx \langle x_{cl}^2 \rangle \sim N^{1/3}. \quad (31)$$

We find that optomechanical systems have the same critical exponents as Dicke and Rabi models [32,34], but a different finite-size scaling. This should not be surprising since all these models have the same type of interaction approximately $(a + a^\dagger)(b + b^\dagger)$ in the exact thermodynamic limit [in the Rabi model the interaction is approximately $(a + a^\dagger)^2$]. In contrast, their nonlinear interactions, which are the central element for deriving the finite scaling, are different (quartic versus cubic).

IV. CONCLUSION AND OUTLOOK

In this paper we showed that driven-dissipative optomechanical systems undergo dissipative phase transitions in the well-defined thermodynamic limit. The system exhibits a rich phase diagram composed of different regions which are separated by DPTs: first- and second-order dissipative phase transitions and periodic orbits.

Some of the first-order DPTs happen in a regime of parameters that are within experimental reach. Our work predicts the observation of the first-order DPT and its characteristics, such as critical slowing down and hysteretic behavior in the laboratory. Furthermore, our theoretical analysis at the thermodynamic limit shows that the optomechanical system is stable in the ultrastrong-coupling regime (more details in II in [43]). This should allow experimental studies to probe the physics related to the ultrastrong coupling, such as the nontrivial ground state [62].

Optomechanical systems do exhibit second-order DPTs with and without bifurcation. The equilibrium counterpart of the second-order DPT without bifurcation cannot be explained by Landau theory and in general it corresponds to the domain of topological phase transitions [63]. This is a novel topic in the context of out-of-equilibrium quantum systems, and our work may help to improve the understanding of the matter.

We conclude with a final remark on the possible relevance of our study to the domain of quantum computing. The fact that the system is infinite dimensional and exhibits multiple steady states may find potential applications in the quantum information process [64].

ACKNOWLEDGMENTS

We thank Joshua Morris for helpful comments. B.D. acknowledges support from the Austrian Science Fund (FWF) through BeyondC-F7112. U.D. and M.A. acknowledge support from FWF Project No. I 5111-N, the European Research Council Grant No. 6 CoG QLev4G, the ERA-NET program QuantERA through grants QuaSeRT and TheBlinQC (via the EC, the Austrian ministries BMDW and BMBWF and research promotion agency FFG), the European Union's Horizon 2020 research and innovation program under Grant No. 863132 (iQLev).

- [1] F. Minganti, A. Biella, N. Bartolo, and C. Ciuti, Spectral theory of Liouvillians for dissipative phase transitions, *Phys. Rev. A* **98**, 042118 (2018).
- [2] A. Carollo, D. Valenti, and B. Spagnolo, Geometry of quantum phase transitions, *Phys. Rep.* **838**, 1 (2020).
- [3] H. J. Carmichael, Analytical and numerical results for the steady-state in cooperative resonance fluorescence, *J. Phys. B* **13**, 3551 (1980).
- [4] M. Žnidarič, Solvable quantum nonequilibrium model exhibiting a phase transition and a matrix product representation, *Phys. Rev. E* **83**, 011108 (2011).
- [5] S. Diehl, A. Tomadin, A. Micheli, R. Fazio, and P. Zoller, Dynamical Phase Transitions and Instabilities in Open Atomic Many-Body Systems, *Phys. Rev. Lett.* **105**, 015702 (2010).
- [6] P. Werner, K. Völker, M. Troyer, and S. Chakravarty, Phase Diagram and Critical Exponents of a Dissipative Ising Spin Chain in a Transverse Magnetic Field, *Phys. Rev. Lett.* **94**, 047201 (2005).
- [7] L. Capriotti, A. Cuccoli, A. Fubini, V. Tognetti, and R. Vala, Dissipation-Driven Phase Transition in Two-Dimensional Josephson Arrays, *Phys. Rev. Lett.* **94**, 157001 (2005).
- [8] S. Morrison, and A. S. Parkins, Dissipation-driven quantum phase transitions in collective spin systems, *J. Phys. B* **41**, 195502 (2008).
- [9] J. Eisert and T. Prosen, Noise-driven quantum criticality, [arXiv:1012.5013](https://arxiv.org/abs/1012.5013).
- [10] M. J. Bhaseen, J. Mayoh, B. D. Simons, and J. Keeling, Dynamics of nonequilibrium Dicke models, *Phys. Rev. A* **85**, 013817 (2012).
- [11] W. Nie, M. Antezza, Y.-x. Liu, and F. Nori, Dissipative Topological Phase Transition with Strong System-Environment Coupling, *Phys. Rev. Lett.* **127**, 250402 (2021).
- [12] E. M. Kessler, G. Giedke, A. Imamoglu, S. F. Yelin, M. D. Lukin, and J. I. Cirac, Dissipative phase transition in a central spin system, *Phys. Rev. A* **86**, 012116 (2012).
- [13] X. H. H. Zhang and H. U. Baranger, Driven-dissipative phase transition in a Kerr oscillator: From semiclassical \mathcal{PT} symmetry to quantum fluctuations, *Phys. Rev. A* **103**, 033711 (2021).
- [14] W. Casteels, R. Fazio, and C. Ciuti, Critical dynamical properties of a first-order dissipative phase transition, *Phys. Rev. A* **95**, 012128 (2017).
- [15] F. Vicentini, F. Minganti, R. Rota, G. Orso, and C. Ciuti, Critical slowing down in driven-dissipative Bose-Hubbard lattices, *Phys. Rev. A* **97**, 013853 (2018).
- [16] P. D. Drummond and D. F. Walls, Quantum theory of optical bistability. I. Nonlinear polarisability model, *J. Phys. A: Math. Gen.* **13**, 725 (1980).
- [17] H. J. Carmichael, Breakdown of Photon Blockade: A Dissipative Quantum Phase Transition in Zero Dimensions, *Phys. Rev. X* **5**, 031028 (2015).
- [18] M.-L. Cai, Z.-D. Liu, W.-D. Zhao, Y.-K. Wu, Q.-X. Mei, Y. Jiang, L. He, X. Zhang, Z.-C. Zhou, and L.-M. Duan, Observation of a quantum phase transition in the quantum Rabi model with a single trapped ion, *Nat. Commun.* **12**, 1126 (2021).
- [19] F. Brennecke, R. Mottl, K. Baumann, R. Landig, T. Donner, and T. Esslinger, Real-time observation of fluctuations at the driven-dissipative Dicke phase transition, *Proc. Natl. Acad. Sci. USA* **110**, 11763 (2013).
- [20] S. R. K. Rodriguez, W. Casteels, F. Storme, N. C. Zambon, I. Sagnes, L. Le Gratiet, E. Galopin, A. Lemaître, A. Amo, C. Ciuti, and J. Bloch, Probing a Dissipative Phase Transition via Dynamical Optical Hysteresis, *Phys. Rev. Lett.* **118**, 247402 (2017).
- [21] J. M. Fink, A. Dombi, A. Vukics, A. Wallraff, and P. Domokos, Observation of the Photon-Blockade Breakdown Phase Transition, *Phys. Rev. X* **7**, 011012 (2017).
- [22] T. Fink, A. Schade, S. Höfling, C. Schneider, and A. Imamoglu, Signatures of a dissipative phase transition in photon correlation measurements, *Nat. Phys.* **14**, 365 (2018).
- [23] M. Fitzpatrick, N. M. Sundaresan, A. C. Li, J. Koch, and A. A. Houck, Observation of a Dissipative Phase Transition in a One-Dimensional Circuit QED Lattice, *Phys. Rev. X* **7**, 011016 (2017).
- [24] S. Barrett, K. Hammerer, S. Harrison, T. E. Northup, and T. J. Osborne, Simulating Quantum Fields with Cavity QED, *Phys. Rev. Lett.* **110**, 090501 (2013).
- [25] M. J. Hartmann, Quantum simulation with interacting photons, *J. Opt.* **18**, 104005 (2016).
- [26] D. G. Angelakis, M. F. Santos, and S. Bose, Photon-blockade-induced Mott transitions and XY spin models in coupled cavity arrays, *Phys. Rev. A* **76**, 031805 (2007).
- [27] A. A. Houck, H. E. Türeci, and J. Koch, On-chip quantum simulation with superconducting circuits, *Nat. Phys.* **8**, 292 (2012).
- [28] A. D. Greentree, C. Tahan, J. H. Cole, and L. C. L. Hollenberg, Quantum phase transitions of light, *Nat. Phys.* **2**, 856 (2006).
- [29] R. Blatt and F. R. Christian, Quantum simulations with trapped ions, *Nat. Phys.* **8**, 277 (2012).
- [30] I. Carusotto and C. Ciuti, Quantum fluids of light, *Rev. Mod. Phys.* **85**, 299 (2013).
- [31] M. J. Hartmann, F. G. S. L. Brandao, and M. B. Plenio, Strongly interacting polaritons in coupled arrays of cavities, *Nat. Phys.* **2**, 849 (2006).
- [32] E. G. Dalla Torre, S. Diehl, M. D. Lukin, S. Sachdev, and P. Strack, Keldysh approach for nonequilibrium phase transitions in quantum optics: Beyond the Dicke model in optical cavities, *Phys. Rev. A* **87**, 023831 (2013).
- [33] C. Emary and T. Brandes, Chaos and the quantum phase transition in the Dicke model, *Phys. Rev. E* **67**, 066203 (2003).
- [34] M.-J. Hwang, P. Rabl, and M. B. Plenio, Dissipative phase transition in the open quantum Rabi model, *Phys. Rev. A* **97**, 013825 (2018).
- [35] M.-J. Hwang and M. B. Plenio, Quantum Phase Transition in the Finite Jaynes-Cummings Lattice Systems, *Phys. Rev. Lett.* **117**, 123602 (2016).
- [36] W. P. Bowen and G. J. Milburn, *Quantum Optomechanics* (CRC, Boca Raton, 2015).
- [37] C. Genes, A. Mari, P. Tombese, and D. Vitali, Robust entanglement of a micromechanical resonator with output optical fields, *Phys. Rev. A* **78**, 032316 (2008).
- [38] G. A. Peterson, S. Kotler, F. Lecocq, K. Cicak, X. Y. Jin, R. W. Simmonds, J. Aumentado, and J. D. Teufel, Ultrastrong Parametric Coupling between a Superconducting Cavity and a Mechanical Resonator, *Phys. Rev. Lett.* **123**, 247701 (2019).
- [39] S. G. Hofer and K. Hammerer, Quantum control of optomechanical systems, *Adv. At. Mol. Opt. Phys.* **66**, 263 (2017).
- [40] F. Minganti, I. I. Arkhipov, A. Miranowicz, and F. Nori, Continuous dissipative phase transitions with or without symmetry breaking, *New J. Phys.* **23**, 122001 (2021).

- [41] M. Aspelmeyer, T. J. Kippenberg, and F. Marquardt, Cavity optomechanics, *Rev. Mod. Phys.* **86**, 1391 (2014).
- [42] U. DeliĆ, M. Reisenbauer, D. Grass, N. Kiesel, V. Vuletić, and M. Aspelmeyer, Cavity Cooling of a Levitated Nanosphere by Coherent Scattering, *Phys. Rev. Lett.* **122**, 123602 (2019).
- [43] See Supplemental Material at <http://link.aps.org/supplemental/10.1103/PhysRevA.107.053505> for details.
- [44] L. Mandel and E. Wolf, *Optical Coherence and Quantum Optics* (Cambridge University Press, Cambridge, 1995).
- [45] E. X. DeJesus and C. Kaufman, Routh-Hurwitz criterion in the examination of eigenvalues of a system of nonlinear ordinary differential equations, *Phys. Rev. A* **35**, 5288 (1987).
- [46] H.-P. Breuer and F. Petruccione, *The Theory of Open Quantum Systems* (Oxford University Press, Oxford, 2002).
- [47] Á. Rivas and S. F. Huelga, *Open Quantum Systems: An Introduction*, Springer Briefs in Physics Vol. 10 (Springer, Berlin, 2012).
- [48] O. Scarlatella, A. A. Clerk, and M. Schiro, Spectral functions and negative density of states of a driven-dissipative nonlinear quantum resonator, *New J. Phys.* **21**, 043040 (2019).
- [49] S. H. Strogatz, *Nonlinear Dynamics and Chaos with Student Solutions Manual: With Applications to Physics, Biology, Chemistry, and Engineering* (CRC, Boca Raton, 2018).
- [50] R. Ghobadi, A. R. Bahrapour, and C. Simon, Quantum optomechanics in the bistable regime, *Phys. Rev. A* **84**, 033846 (2011).
- [51] N. Lörch, J. Qian, A. Clerk, F. Marquardt, and K. Hammerer, Laser Theory for Optomechanics: Limit Cycles in the Quantum Regime, *Phys. Rev. X* **4**, 011015 (2014).
- [52] P. D. Nation, Nonclassical mechanical states in an optomechanical micromaser analog, *Phys. Rev. A* **88**, 053828 (2013).
- [53] F. Marquardt, J. G. E. Harris, and S. M. Girvin, Dynamical Multistability Induced by Radiation Pressure in High-Finesse Micromechanical Optical Cavities, *Phys. Rev. Lett.* **96**, 103901 (2006).
- [54] T. F. Roque, F. Marquardt, and O. M. Yevtushenko, Nonlinear dynamics of weakly dissipative optomechanical systems, *New J. Phys.* **22**, 013049 (2020).
- [55] R. Simon, Peres-Horodecki Separability Criterion for Continuous Variable Systems, *Phys. Rev. Lett.* **84**, 2726 (2000).
- [56] G. Adesso, A. Serafini, and F. Illuminati, Extremal entanglement and mixedness in continuous variable systems, *Phys. Rev. A* **70**, 022318 (2004).
- [57] R. Simon, N. Mukunda, and B. Dutta, Quantum-noise matrix for multimode systems: $U(n)$ invariance, squeezing, and normal forms, *Phys. Rev. A* **49**, 1567 (1994).
- [58] N. Goldenfeld, *Lectures on Phase Transitions and the Renormalization Group* (CRC, Boca Raton, 2018).
- [59] B. Horstmann, J. I. Cirac, and G. Giedke, Dissipative dynamics and phase transitions in fermionic systems, *Phys. Rev. A* **87**, 012108 (2013).
- [60] L. M. Sieberer, M. Buchhold, and S. Diehl, Keldysh field theory for driven open quantum systems, *Rep. Prog. Phys.* **79**, 096001 (2016).
- [61] A. Kamenev, in *Nanoscopic Quantum Transport, Proceedings of the Les Houches Summer School of Theoretical Physics, LXXXI, 2004*, edited by H. Bouchiat, Y. Gefen, S. Guéron, G. Montambaux, and J. Dalibard (Elsevier, Amsterdam, 2005), Vol. 81, pp. 177–246.
- [62] P. Forn-Díaz, L. Lamata, E. Rico, J. Kono, and E. Solano, Ultrastrong coupling regimes of light-matter interaction, *Rev. Mod. Phys.* **91**, 025005 (2019).
- [63] J. M. Kosterlitz and D. J. Thouless, Ordering, metastability and phase transitions in two-dimensional systems, *J. Phys. C* **6**, 1181 (1973).
- [64] M. Mirrahimi, Z. Leghtas, V. V. Albert, S. Touzard, R. J. Schoelkopf, L. Jiang, and M. H. Devoret, Dynamically protected cat-qubits: A new paradigm for universal quantum computation, *New J. Phys.* **16**, 045014 (2014).